

Research Article

Extruded Catalysts with Magnetic Properties for Biodiesel Production

Euripedes Garcia Silveira Junior ¹, Oselys Rodriguez Justo ², Victor Haber Perez ¹,
Inés Reyero ³, Ana Serrano-Lotina ⁴, Leonardo Campos Ramirez ¹,
and Dayana F. dos Santos Dias ¹

¹Process Engineering Sector, Center of Science and Agropecuary Technology, State University of the Northern of Rio de Janeiro, Rio de Janeiro, Brazil

²Environmental School, Estácio de Sá University, Campos dos Goytacazes, RJ, Brazil

³Department of Science, Public University of Navarre, Campus of Arrosadía, Pamplona, Spain

⁴Institute of Catalysis and Petrochemistry (CSIC), Campus Universidad Autónoma de Madrid, Madrid, Spain

Correspondence should be addressed to Victor Haber Perez; victorhaberper@gmail.com

Received 28 August 2018; Revised 16 November 2018; Accepted 25 November 2018; Published 30 December 2018

Academic Editor: Peter Majewski

Copyright © 2018 Euripedes Garcia Silveira Junior et al. This is an open access article distributed under the Creative Commons Attribution License, which permits unrestricted use, distribution, and reproduction in any medium, provided the original work is properly cited.

The aim of this work was to evaluate the performance of different extruded catalysts containing K_2CO_3 as active phase and adding conveniently $\gamma-Al_2O_3$ and/or sepiolite and magnetic particles on the biodiesel production from sunflower oil by the ethanolic route. Firstly, the content of the Fe_3O_4 on the catalyst (0.1, 0.2, 0.3, and 0.4 g Fe_3O_4 /g of $K_2CO_3/\gamma-Al_2O_3$), after calcination step, was evaluated to verify the separation facility of the catalysts with magnetic properties from reactional medium, using an external magnetic field, at the end of biodiesel synthesis. After that, three different catalysts were considered for comparative purposes: (a) $K_2CO_3/\gamma-Al_2O_3$; (b) $K_2CO_3/\gamma-Al_2O_3/Fe_3O_4$; (c) $K_2CO_3/\gamma-Al_2O_3/Sepiolite/Fe_3O_4$ and subsequently characterized by dynamometry, TGA, SEM, VSM, BET, and XRD to determine their mechanical, structural, magnetic, and textural properties. However, their catalytic activities were determined through biodiesel production that was carried out in a glass volumetric reactor during 4 h, under magnetic stirring with 5% wt. of the catalyst and oil : ethanol molar ratio (1 : 12) at 80°C reaction temperature. The best result, i.e., around 88% of biodiesel conversion, was obtained with catalyst $K_2CO_3/\gamma-Al_2O_3/Sepiolite/Fe_3O_4$ which showed also satisfactory textural and mechanical strength properties comparatively with the other catalytic derivatives. In addition, no agglomeration of the particles was observed during the reaction, and the magnetic property of this catalytic system was satisfactory for adequate separation from reactional medium seeking further reuse. The attained results are attractive for possible implementation at industrial scale and can be considered to mitigate drawbacks which resulting by using of homogeneous catalysts in the conventional processes.

1. Introduction

The search for alternatives to mitigate global warming is currently a major global challenge. In this context, biodiesel is a biofuel with great potential. Brazil is the second largest producer of biodiesel in the world, with 51 biodiesel plants producing around 21000 m³/day [1] to use in diesel/biodiesel blends (with a volumetric ratio 90/10%) accordingly approved

by the National Energy Policy Council (CNPE) of the Ministry of Mines and Energy [2].

Basically, in Brazil, the conventional biodiesel production at industrial scale is carried out by chemical transesterification by homogeneous catalysis and using methanol as reactant alcohol although there are some plants that produce ethanolic biodiesel [3]. The predominant feedstock is soybean oil, which corresponds to 64.84% of the

national production, followed by beef tallow with 15.50% and finally other raw materials, such as pork fat, palm oil, and various fatty sources which represent 19.66% [1]. In this scenario, attention must be paid to two important aspects in this conventional process that lead to technological and/or environmental problems which have already been reported: (a) the use of homogeneous catalysts and (b) the use of methanol as a reactant alcohol [3, 4]. In the first case, the catalyst solubilizes in the reaction medium preventing its reuse and, therefore, this makes the process more expensive. In addition, soap forms when oils with high content of free fatty acids are used, resulting in more difficult and additional steps of washing the biodiesel for the removal of salts, glycerol and impurities. Acid or basic wastewater also needs treatment of the generated effluent [5, 6]. In the second case, it should be emphasized that methanol usually comes from natural gas (a fossil resource). Particularly, Brazil has mitigated this problem by implementing the use of bioethanol in the production of biodiesel. Bioethanol is conventionally produced on a large scale by a biotechnology way, around 28611.04×10^3 L/year of both anhydrous and hydrated ethanol in 2017 [7], thus making biodiesel production a renewable totally process.

A technological strategy that has received special attention is the use and development of heterogeneous catalysts for the production of biodiesel, since these can sometimes be prepared in simple form, present great potential for reuse, and in some cases low cost [8, 9]. In this context, basic catalytic derivatives [10–12], acids [13–16], bifunctional systems [17, 18], and enzymatic derivatives, which has shown excellent performance despite the high commercial cost of the purified enzymes [19, 20], have been evaluated.

Despite the advantages of heterogeneous catalysts, there are difficulties, because in some cases these catalysts are very fine powders, which in addition to forming agglomerates during the reaction, part of the catalyst is lost in the separation processes, thus limiting their applications at industrial scale [21].

In this context, the magnetic nanoparticles are particularly attractive as additives to the supports are used for the heterogeneous catalysts due to their advantages of fast and facile catalyst separation from the reaction mixture by applying an external magnetic field, thereby eliminating process steps such as conventional centrifugation and filtration [22]. However, the magnetic nanoparticles forming particle clusters may restrict the dispersion of the nanoparticles in the reaction mixture due to their magnetic dipole-dipole attraction [22].

Catalysts with magnetic properties have been studied in the biodiesel production [23–31]. However, information in the literature on the application of the magnetic properties of these catalysts is still scarce. The studies mention only the removal of the catalyst from the reaction medium by centrifugation [30], filtration [26], or magnetic separation using magnets [23–25, 27–29, 31]. It is worth mentioning that in some cases, magnetically stabilized bed reactors are used, a system that allows catalysts with magnetic properties [32–35] under the action of a magnetic field to be aligned axially and/or transversely within the reactor.

Thus, the aim of this work was to evaluate extruded catalysts with cylindrical geometry (pellets) based on $K_2CO_3/\gamma-Al_2O_3$ /sepiolite containing magnetic particles (Fe_3O_4) in order to verify their potential in the biodiesel production by ethanolic transesterification route.

2. Materials and Methods

2.1. Materials. The used feedstock for biodiesel production was commercial sunflower oil. A mixture C4-C24 of fatty acid ethyl esters (FAEEs) was used as standard for biodiesel characterization (SUPELCO). Boehmite (PURAL SB SASOL containing 85% of Al_2O_3) was used as $\gamma-Al_2O_3$ (alumina) precursor; CH_4N_2O (urea) and sepiolite (Pansil 100, 60% purity) ($Mg_4Si_6O_{15}(OH)_2 \cdot 6H_2O$) from TOLSA S.A. (Spain) were used conveniently as temporary and permanent binders, respectively. Iron chloride II (ALFA AESAR), iron chloride III (Sigma-Aldrich), and sodium hydroxide (Sigma-Aldrich) were used for magnetic particle synthesis. Potassium carbonate (SCHARLAU) was used as active phase component, and ethanol P.A. (SCHARLAU) was used as reagent alcohol.

2.2. Experimental Methods

2.2.1. Synthesis of Magnetic Particles. Magnetic nanoparticles were prepared by the coprecipitation method. For the synthesis of the magnetite, 3.597 g of $FeCl_2$ and 6.488 g of $FeCl_3$ were diluted in deionized water; a solution of sodium hydroxide (6.4 g) was added dropwise until the pH of the solution was adjusted to 11; and the solution was stirred vigorously at $80^\circ C$. After synthesis, the magnetic nanoparticles were filtered and washed with deionized water to remove the chloride ions and then washed with ethanol to ensure the removal of the entire residue from the synthesis. Finally, the nanoparticles were dried in a vacuum oven at $80^\circ C$ for 24 h.

2.2.2. Procedure for Preparation of Catalysts. Three different catalyst groups were prepared for comparative purpose: (a) the first one without magnetic particles was prepared by mixing 1.75 g of K_2CO_3 , 4.977 g of boehmite, and 15% wt. urea; (b) the second group was prepared by mixing 1.75 g of K_2CO_3 , 4.977 g of boehmite, and 15% wt. urea and adding several magnetite contents: 0.1, 0.2, 0.3, and 0.4 g Fe_3O_4/g of ($K_2CO_3/\gamma-Al_2O_3$); and (c) the third catalyst was prepared with 1.75 g of K_2CO_3 , 4.002 g of $\gamma-Al_2O_3$, and 0.975 g of sepiolite, but containing just 0.3 g of Fe_3O_4/g of catalyst ($K_2CO_3/\gamma-Al_2O_3$ /sepiolite).

In all cases, the component mixtures were milled to homogenize the particle sizes and water was added dropwise to form a homogeneous mass and extrusion was carried out using a syringe device. Then, the catalysts were previously dried at $105^\circ C$ for 16 hours to reduce their moisture content and finally calcined at $500^\circ C$ for 4 hours.

2.2.3. Characteristics of the Reactor Assisted by Magnetic Field. The reactor coupled with an electromagnetic field generator was operated to separate the catalysts with

magnetic properties using magnetic field flux density around 20 mT and field lines oriented conveniently to the axial/transversal direction with respect to the vertical axis of the bioreactor. The magnetic field flux density was monitored by a GM08 gaussmeter (Hirst Magnetic Instruments Ltd., United Kingdom).

2.2.4. Procedure for Biodiesel Production. The biodiesel production was carried out by transesterification through the ethanolic route. In each experiment, 5% wt. of catalyst in relation to oil mass was used, whereas the oil : alcohol molar ratio was 1 : 12. The reactions were conducted in a glass-jacketed reactor coupled to a thermostatic bath to adjust the reactor temperature at 80°C during 4 h reactional time. Then, the reaction was stopped, catalysts separated by magnetic field, and the formed biodiesel was purified as described previously in [4] for further characterization.

2.3. Analytical Methods

2.3.1. Gas Chromatography (GC). The formed biodiesel was monitored by gas chromatography using a Bruker GC model 430-GC. The injector and detector temperatures were set at 250°C. Helium was used as the carrier gas with a flow of 312.3 mL/min of entrainment gas at a linear velocity of 62.0 cm/min. The column temperature was kept at 50°C for 1 min, heated to 180°C at 15°C/min, then to 300°C at 7°C/min, and maintained constant for 10 min. The detector temperature was 250°C, and the chromatographic column used was a Bruker BR 5 MS (30 m × 0.25 mm × 0.25 μm) with 5% diphenyl and 95% dimethyl polysiloxane composition. Identification and quantification of formed biodiesel were carried out according to the calibration curve prepared using FAEs (referent to the fatty acids contained in the sunflower oil) at four concentrations and ethyl decanoate as internal standard (Sigma-Aldrich).

2.3.2. Mechanical Strength. The mechanical strength of the catalysts was measured in terms of burst pressure using a Chatillon, LTMC model dynamometer. The tests consisted on determining the pressure needed to be applied on the external surface of the catalyst to cause its rupture [36].

2.3.3. Magnetization Measurements by Vibrating-Sample Magnetometer (VSM). The magnetic properties of the particles and magnetic catalysts were performed on a SQUID vibrating-sample magnetometer (Quantum Design® models MPMS 57, MPMS 7T). The temperature and field dependence of the samples were recorded on a Quantum Design MPMS-XL superconducting quantum interference device (SQUID). ZFC/FC measurements were performed in the 0–330 K temperature range with an applied field of 10000 Oe.

2.3.4. Thermogravimetric Analysis (TG/DTG). Simultaneous thermogravimetric and differential thermal analyses (TGA-DTA) of catalysts were carried out in a flowing air

atmosphere using an analyzer (STA 6000) equipped with a gas cell (PerkinElmer). Around 30 mg of sample was placed in a Pt/Rh crucible and heated up to 950°C with a heating rate of 10°C/min.

2.3.5. Scanning Electron Microscopy (SEM). SEM micrographs of the catalyst were obtained on a scanning electron microscope (HITACHI TM1000 tabletop microscope model). The procedure for preparing the materials for analysis consisted of depositing a portion of the solid onto a carbon adhesive tape affixed to the sample holder. The micrographs were obtained with magnifications ranging from 100 to 3000×.

2.3.6. Textural Characterization. Specific surface area data were calculated from nitrogen adsorption/desorption isotherms obtained at -196°C in an ASAP 2420 apparatus (Micromeritics), after application of the BET equation [37, 38].

2.3.7. X-Ray Diffraction. Analysis of the powder (support and/or catalysts) obtained by previous milling was performed by X-ray diffractometry (XRD, X'Pert PRO theta/2theta, PANalytical, the Netherlands). The patterns were recorded over the angular range of 5–80° (2θ) with a step size of 0.0334° and a time per step of 100 seconds, using Cu Kα radiation (λ = 0.154056 nm) with a working voltage and current of 40 kV and 100 mA, respectively.

3. Results and Discussion

Initially, VSM magnetization measurements were performed for each catalytic system prepared (Table 1). As it can be observed, there were increases up to 4 times in the magnetization value (around 3 to 13 emu/g) when the magnetite content added to the prepared derivatives increased from 0.1 to 0.4 g/g of K₂CO₃/γ-Al₂O₃. However, a fluid dynamics analysis of this catalyst with magnetic properties performed in the magnetic field reactor, illustrated in Figure 1, showed that the catalyst containing 0.3 g Fe₃O₄/g of K₂CO₃/γ-Al₂O₃ was the most suitable for magnetically stabilizing the particle bed. In this condition, it is possible to guarantee the separation of the catalyst from the reaction medium when the biodiesel formation is completed.

In addition, the catalytic activity of the developed catalysts was measured by the transesterification reactions for biodiesel formation (Figure 2), carried out according to the conditions previously described. In this context, the kinetic results of the transesterification reaction (Figure 2) revealed that in all cases biodiesel formation occurred independently of the Fe₃O₄ content in the catalyst, showing the best results when 0.3 g Fe₃O₄/g of K₂CO₃/γ-Al₂O₃ was used (Table 1). All the samples showed mechanical deficiencies that resulted in partial or total rupture in some samples. This fact can be attributed to the use of CH₄N₂O as binder in the preparation of these catalytic derivatives, because this compound

TABLE 1: Magnetic properties and yield of sunflower biodiesel produced by the catalysts.

Catalysts	Magnetization (emu/g)	Biodiesel yield (%)
$K_2CO_3/\gamma-Al_2O_3$	0.00	65.73
$K_2CO_3/\gamma-Al_2O_3/(0.1)Fe_3O_4$	3.31	
$K_2CO_3/\gamma-Al_2O_3/(0.2)Fe_3O_4$	7.60	69.22
$K_2CO_3/\gamma-Al_2O_3/(0.3)Fe_3O_4$	10.08	78.86
$K_2CO_3/\gamma-Al_2O_3/(0.4)Fe_3O_4$	13.46	70.82

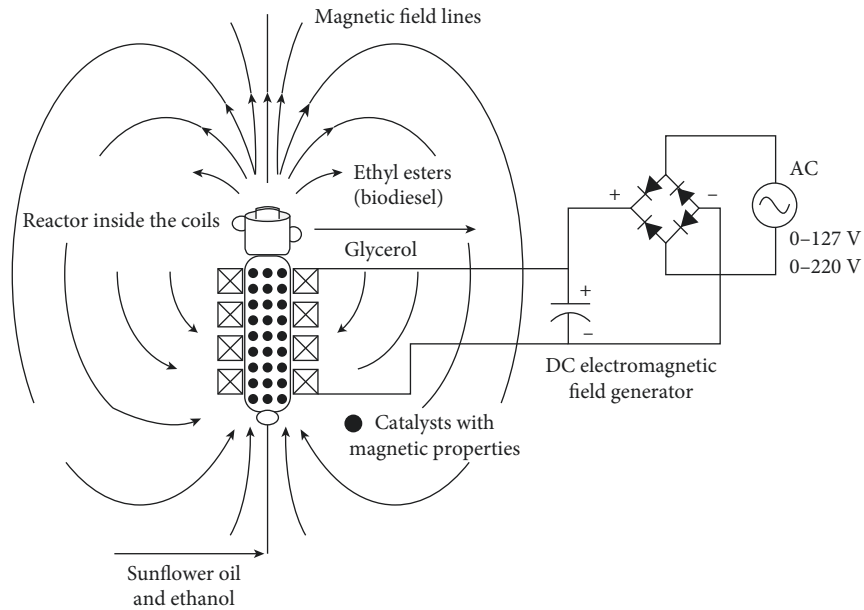


FIGURE 1: Experimental setup of the chemical reactor assisted by magnetic field for catalysts (with magnetic properties) separation from reactional medium at the end of the biodiesel synthesis.

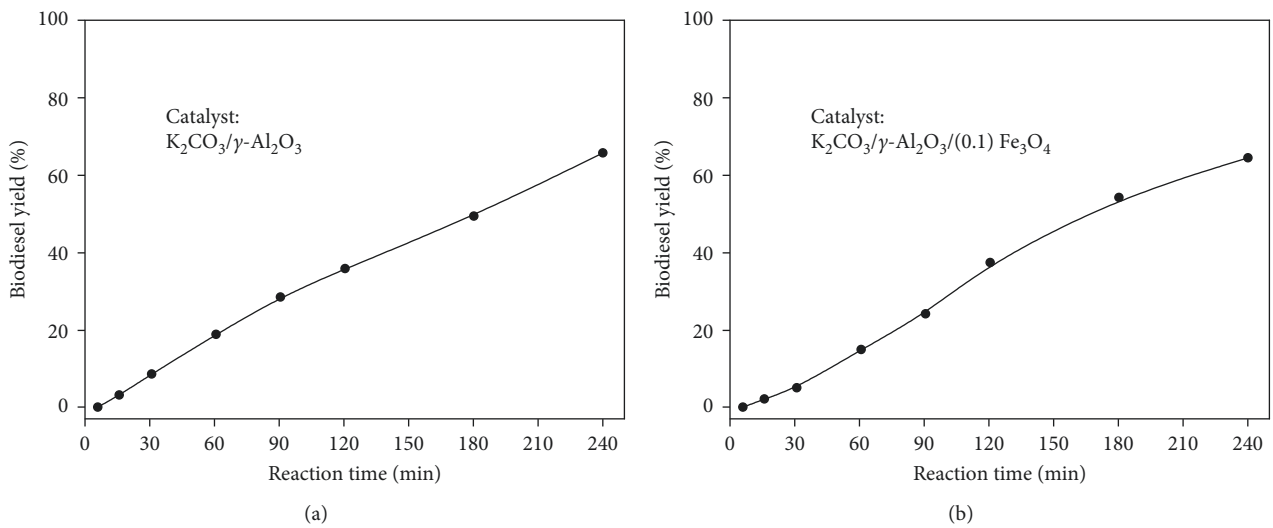


FIGURE 2: Continued.

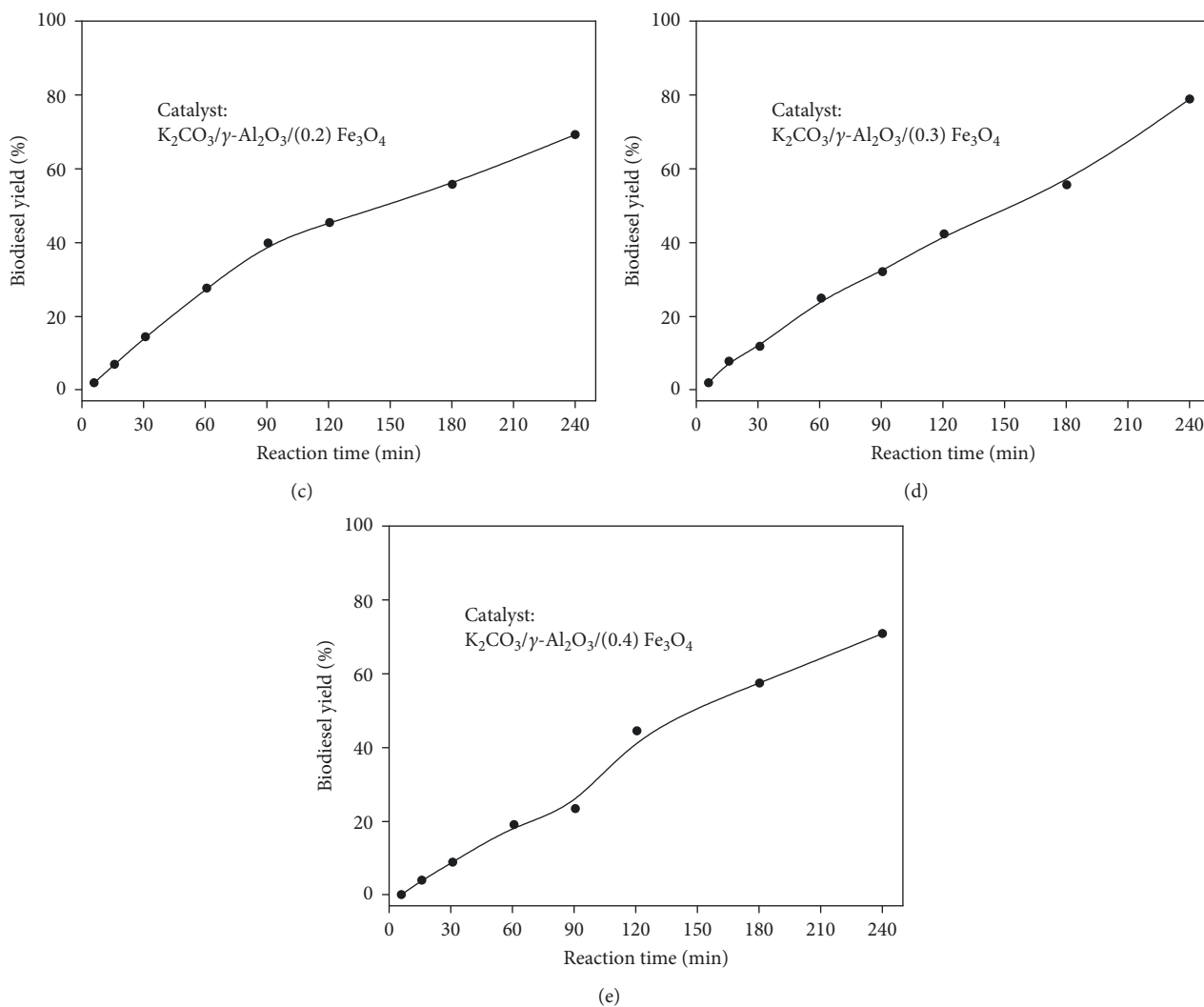


FIGURE 2: Biodiesel production yield from sunflower oil and ethanol using catalysts containing different quantities of Fe_3O_4 in their structure: (a) $\text{K}_2\text{CO}_3/\gamma\text{-Al}_2\text{O}_3$; (b) $\text{K}_2\text{CO}_3/\gamma\text{-Al}_2\text{O}_3/(0.1) \text{Fe}_3\text{O}_4$; (c) $\text{K}_2\text{CO}_3/\gamma\text{-Al}_2\text{O}_3/(0.2) \text{Fe}_3\text{O}_4$; (d) $\text{K}_2\text{CO}_3/\gamma\text{-Al}_2\text{O}_3/(0.3) \text{Fe}_3\text{O}_4$; (e) $\text{K}_2\text{CO}_3/\gamma\text{-Al}_2\text{O}_3/(0.4) \text{Fe}_3\text{O}_4$.

decomposes during the calcination, thus altering the textural and physicochemical properties of these catalytic systems.

In order to improve the mechanical properties of the catalysts, a new catalyst containing K_2CO_3 was supported on $\gamma\text{-Al}_2\text{O}_3$ with 0.3 g Fe_3O_4 , but sepiolite was added as the binder instead of urea. In this context, Figure 3 shows the kinetic curves of biodiesel formation under the same reaction conditions previously described, but different catalytic derivatives under study were compared: (a) $\text{K}_2\text{CO}_3/\gamma\text{-Al}_2\text{O}_3$; (b) $\text{K}_2\text{CO}_3/\gamma\text{-Al}_2\text{O}_3/(0.3)\text{Fe}_3\text{O}_4$; and (c) $\text{K}_2\text{CO}_3/\gamma\text{-Al}_2\text{O}_3/\text{sepiolite}/(0.3) \text{Fe}_3\text{O}_4$. In this case, it was possible to verify that the catalytic performance of the derivative containing sepiolite resulted in a higher biodiesel formation, compared to the other two cases, reaching around 88% yield in 4 hours of reaction. This result was corroborated by their mechanical, physicochemical, and textural properties as shown in Tables 2 and 3 and Figures 2–4, respectively.

Regarding the mechanical properties, the $\text{K}_2\text{CO}_3/\gamma\text{-Al}_2\text{O}_3$ derivative containing sepiolite showed good results

reaching around $3.92 \pm 0.14 \text{ kgf/cm}$ (Table 2). According to Yamadaya et al. [39], the mechanical strength of pellets prepared from some impregnated alumina is higher than for those prepared from pure alumina. In fact, it is well known that the mechanical strength is a very important property which can affect the activity of extrudate catalysts. However, below 10000 kg/cm^2 of extrusion pressure, the mechanical strength of the pellets is mainly affected by the conditions of preparation of the starting materials, i.e., the content of water and/or particle size of the powder, more than by the extrusion conditions [39]. In this way, it is possible to explain comparatively between the developed catalysts, why when adding sepiolite as a permanent additive in the formulation of the catalyst $\text{K}_2\text{CO}_3/\gamma\text{-Al}_2\text{O}_3/\text{sepiolite}/(0.3) \text{Fe}_3\text{O}_4$, it presented a satisfactory mechanical strength, without decomposing during the biodiesel production. In this case, the presence of clusters or the breaking of extruded pellets was not observed. Thus, it is possible to conclude that sepiolite has good rheological properties and when it acts as

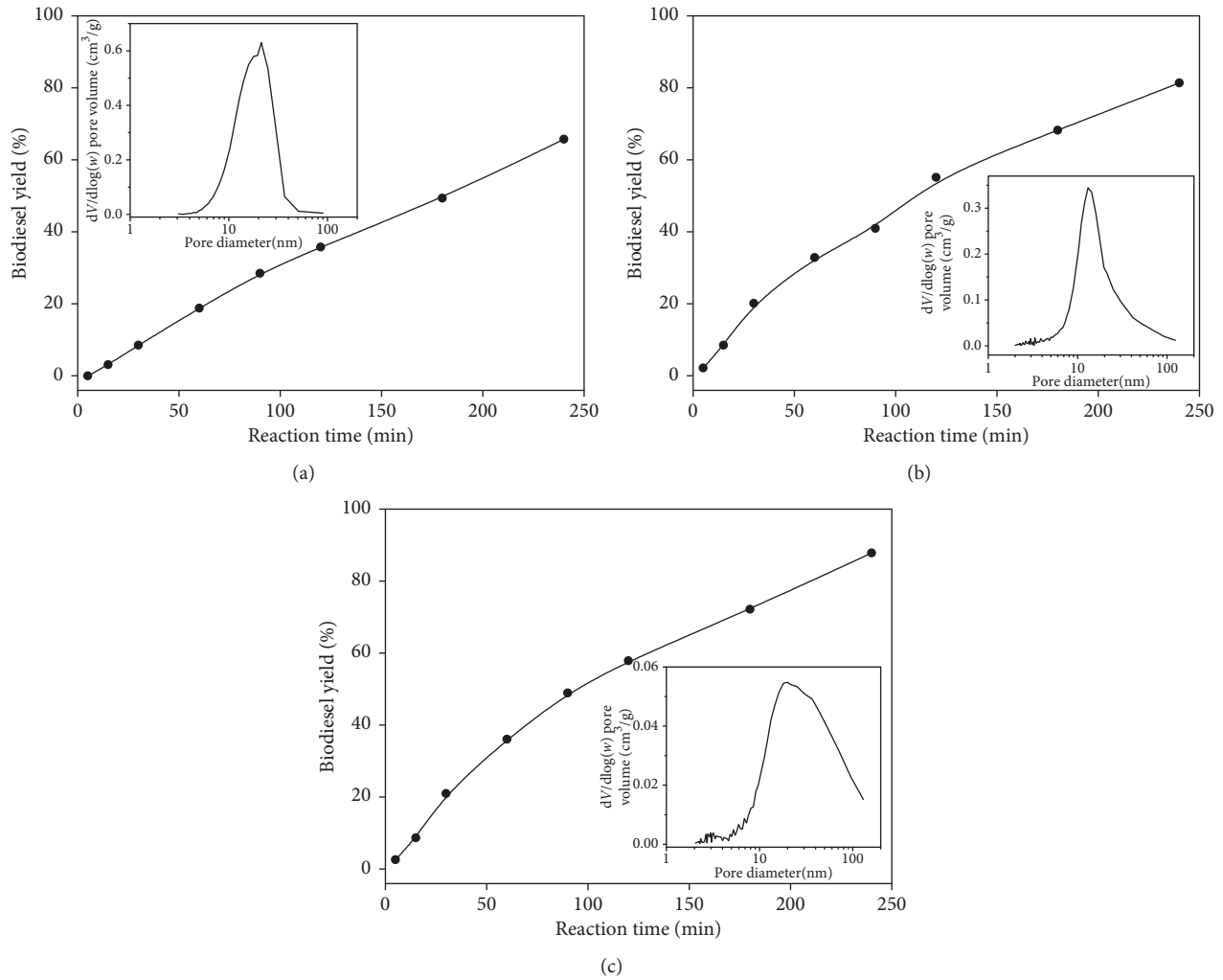


FIGURE 3: Ethanolic sunflower biodiesel production of catalysts: (a) $K_2CO_3/\gamma-Al_2O_3$, (b) $K_2CO_3/\gamma-Al_2O_3/(0.3)Fe_3O_4$, and (c) $K_2CO_3/\gamma-Al_2O_3/sepiolite/(0.3)Fe_3O_4$, under reaction conditions: 5 wt.% mass of extruded catalyst, oil:ethanol molar ratio 1:12, 80°C, 200 rpm, and 4 h reaction time.

TABLE 2: Mechanical strength of the magnetic catalysts after calcination at 500°C.

Catalysts	Geometric property of the particles	Mechanical strength
	Length (mm)	Pressure (kgf/cm)
$K_2CO_3/\gamma-Al_2O_3/(0.3)Fe_3O_4$	4.20 ± 0.50	0.0
$K_2CO_3/\gamma-Al_2O_3/sepiolite/(0.3)Fe_3O_4$	4.84 ± 0.58	3.92 ± 0.14

a binder, there appears to be no need to add any other binder additive.

Figure 4 shows the thermogravimetric analysis for the boehmite, sepiolite, and prepared catalysts. In the boehmite case, this analysis was interesting to evaluate the most adequate calcination temperature for the extruded support preparation, in order to obtain the gamma phase of alumina and the complete binder decomposition when CH_4N_2O is used. Thus, the curve (Figure 4(a)) shows three

TABLE 3: Textural properties for supports and catalysts with magnetic properties.

Catalysts	Textural properties		
	Specific area (m²/g)	Pore volume (cm³/g)	Pore size (nm)
$K_2CO_3/\gamma-Al_2O_3$	65	0.28	16.1
$K_2CO_3/\gamma-Al_2O_3/(0.3)Fe_3O_4$	45	0.16	14.3
$K_2CO_3/\gamma-Al_2O_3/sepiolite/(0.3)Fe_3O_4$	10	0.05	21.4

stages of weight loss at different temperatures. The first two stages of weight loss (first one up to 100°C and the other one around 200°C) can be attributable to loss of free water and absorbed water on the surface, as can be confirmed by the DTA curve, respectively. While the third stage around 450°C is due to the loss of structural water, i.e., referent to decomposition of structural -OH groups, and consequently, there is a phase change from boehmite to $\gamma-Al_2O_3$ formation.

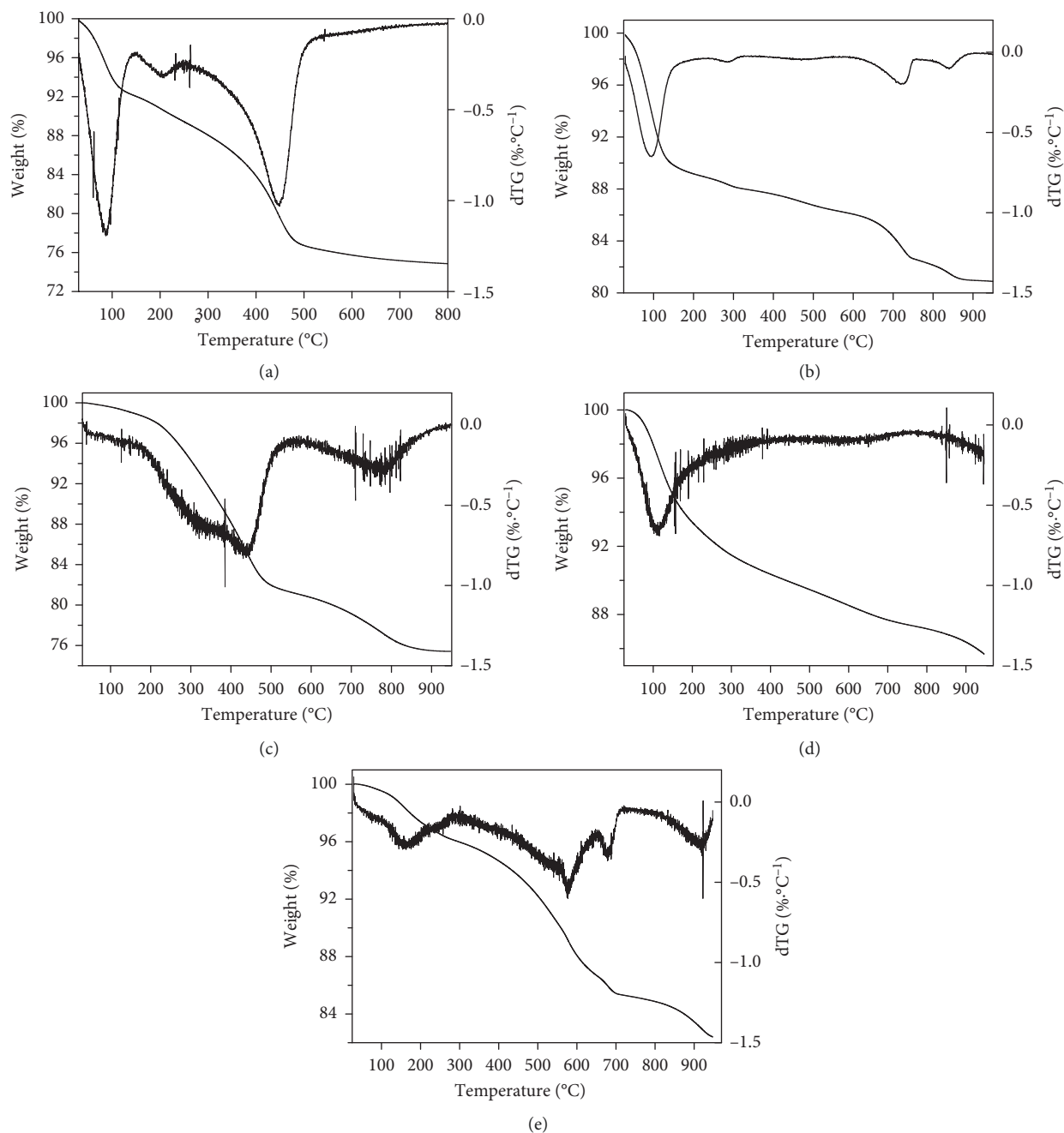


FIGURE 4: Thermogravimetric analysis (TGA-DTG) for (a) boehmite, (b) sepiolite, (c) $K_2CO_3/\gamma-Al_2O_3$, (d) $K_2CO_3/\gamma-Al_2O_3/(0.3)Fe_3O_4$, and (e) $K_2CO_3/\gamma-Al_2O_3/sepiolite/(0.3)Fe_3O_4$.

After 500°C, the material does not change. In this case, 500°C may be considered as the calcination temperature sufficient for the preparation of the carrier without the presence of the additive binder. These results can be corroborated according to the reported data by Chandradass and Balasubramanian [40] that observed similar weight losses between 250 and 500°C.

Figure 4(b) shows TGA/DTA curves for sepiolite ($Mg_4Si_6O_{15}(OH)_2 \cdot 6H_2O$). In this case, the weight loss observed between 100 and 300°C can be attributable to water loss. Over 700°C, another degradation stage can be observed

probably due to sepiolite anhydrite dehydroxylation. Finally, over 800°C sepiolite can be transformed in enstatite. Dehydration and dihydroxylation of sepiolite have been reported in the literature by several authors [41–43].

In a similar way, TGA/DTA curves shown in Figures 4(c)–4(e) were important to verify the thermal stability of the prepared catalysts. In fact, these catalytic systems were developed for biodiesel production at reaction temperatures up to 80°C. Thus, no structural change should be observed at temperatures below 100°C. In addition, the active phase (K_2CO_3) remains in its integral form up to

800°C, confirm by this way the thermal stability of these catalysts.

On the other hand, SEM analysis (Figures 5(a) and 5(b)) revealed comparatively morphological differences between the prepared catalysts containing or no sepiolite. In the micrograph for the catalyst $K_2CO_3/\gamma-Al_2O_3/(0.3)Fe_3O_4$ (Figure 5(a)), it is possible to verify irregular cavities on the catalyst surface. Probably, this is a consequence of the used binder decomposition (CH_4N_2O) during calcination at 500°C. However, for $K_2CO_3/\gamma-Al_2O_3/sepiolite/(0.3)Fe_3O_4$, after calcination, Figure 5(b) shows its morphology in a modified way; i.e., a more regular surface without larger cavities, probably in this case sepiolite which was used as a permanent binder, allowed to obtain a much better mechanical strength as discussed previously. In addition, for the last catalyst, EDS analysis was carried out just to validate its composition, corroborating the following element content: sepiolite (3.5% magnesium and 3% silicon); magnetite (22.9% iron); aluminum (49.9%); and potassium (20.7%).

The textural properties of the catalysts $K_2CO_3/\gamma-Al_2O_3$, $K_2CO_3/\gamma-Al_2O_3/(0.3)Fe_3O_4$ and $K_2CO_3/\gamma-Al_2O_3/sepiolite/(0.3)Fe_3O_4$ are shown in Table 3. The addition of Fe_3O_4 leads to a decrease of the surface area, and with sepiolite the decay is greater. Pore volume follows the same trend. However, when sepiolite is added, the pore size increases substantially (Table 3), suggesting a typical macroporous structure in accordance with the pore distribution shown in Figure 3(c).

On the other hand, the addition of sepiolite as a binder in the catalyst, besides favoring its mechanical strength, also contributed to the increase of its catalytic activity as a function of the pore size increase (Figure 3). However, studies evaluating the influence of sepiolite as a binder on the activity of catalysts based on mixed oxides [44, 45] reported negative effects on its performance with increasing the content of this clay in the catalyst preparation, pointing to the fact that high contents of sepiolite strongly masked the catalyst activity probably due to morphology alterations and increase of the average particle size.

The XRD patterns of Fe_3O_4 , $\gamma-Al_2O_3$, and sepiolite are shown in Figures 6(a)–6(c). Diffractograms of $K_2CO_3/\gamma-Al_2O_3/(0.3)Fe_3O_4$ and $K_2CO_3/\gamma-Al_2O_3/sepiolite/(0.3)Fe_3O_4$ are presented in Figures 6(d) and 6(e). The catalyst $K_2CO_3/\gamma-Al_2O_3/(0.3)Fe_3O_4$ has diffraction peaks corresponding to Fe_3O_4 (JCPDS #19–0629), Al_2O_3 (JCPDS #46–1212), and the compound K–Al–O (JCPDS #39–0050) that represent the active phase of the catalyst identified in the region 2θ : 26–32°. In the case of the catalyst $K_2CO_3/\gamma-Al_2O_3/sepiolite/(0.3)Fe_3O_4$, peaks related to Fe_3O_4 , Al_2O_3 , and sepiolite (JCPDS #34–1216) were also found. The active phase of the catalyst ($KAlSiO_4$) has also been identified in the region 2θ : 26–32° (JCPDS #31–0965).

Finally, according to the biodiesel production results described above, some comments on the use of catalytic derivatives with magnetic properties are relevant. Several published works have reported good yields in biodiesel production and catalyst recovery facilities when using catalysts with magnetic properties [27, 46, 47]. In some of these cases, the catalysts showed good magnetic properties; for example, Liu et al. [27] synthesized a basic magnetic

derivative ($MgFe_2O_4@CaO$) which presented 48.6°emu/g of magnetization. Similarly, Wu et al. [46] synthesized $S_2O_8^{2-}/ZrO_2-TiO_2-Fe_3O_4$ to produce biodiesel and obtained a catalyst with saturation magnetization of 21 emu/g. In addition, Tang et al. [47] synthesized CaO/Fe_3O_4 to produce biodiesel; however, this catalyst, compared with the previous cases, showed low magnetization around 6.34 emu/g but apparently was also sufficient to separate the catalyst. Particularly in our case, the catalyst $K_2CO_3/\gamma-Al_2O_3/sepiolite/(0.3)Fe_3O_4$ presented magnetization of 5.74 emu/g, which was adequate to interact with external field and enabled its removal from the reactional medium, aiming at reusing it in future studies.

On the other hand, in some cases cited in the literature, the authors have carried out the magnetic characterization of the catalysts. However, they only allude to the purpose or the fact of removing the magnetic catalyst from the reactional medium using an external magnetic field generated by permanent magnets but often without any specification of their magnetic properties [23, 46, 47]. In other cases, even when catalysts with magnetic particles are used, they have been removed from the reaction medium by conventional unitary operations such as centrifugation and filtration, among others [26, 30] without any technological justification for the use of these catalytic derivatives with magnetic properties.

Heterogeneous catalysts in powder [11–14] have been extensively studied, showing good yields of biodiesel conversion. However, as is known, these systems frequently present problems of agglomeration in the reaction medium, making it difficult to remove them at the end of the reaction for their subsequent reuse. In this context, extruded catalysts can mitigate this technological problem. Table 4 shows some studies in which extruded catalysts were used satisfactorily in biodiesel production.

As can be observed, compared to the studies reported in Table 4, the results presented in our work can be considered satisfactory, since only one reaction step was enough to achieve 88% yield, which could easily reach complete conversion with an additional reaction step, as happens strategically in industrial-scale processes.

4. Conclusions

Magnetic extruded catalysts based on K_2CO_3 , $\gamma-Al_2O_3$, sepiolite, and magnetite particles were prepared to catalyze the biodiesel formation by transesterification of sunflower oil. The best results were obtained when $K_2CO_3/\gamma-Al_2O_3/sepiolite/(0.3)Fe_3O_4$ was used as a catalyst in the transesterification reaction, reaching a yield in ethanolic biodiesel around 88% at the reaction end. Also, magnetic separation can be a good alternative to separate a magnetic catalyst after each reaction step, guaranteeing a high recovery for its further reuse in several cycles. Thus, this heterogeneous catalyst can be considered as an attractive alternative, with respect to the homogeneous catalysts, for biodiesel production. Nevertheless, further technoeconomic studies must be carried out to verify its viability for the biodiesel production at industrial scale.

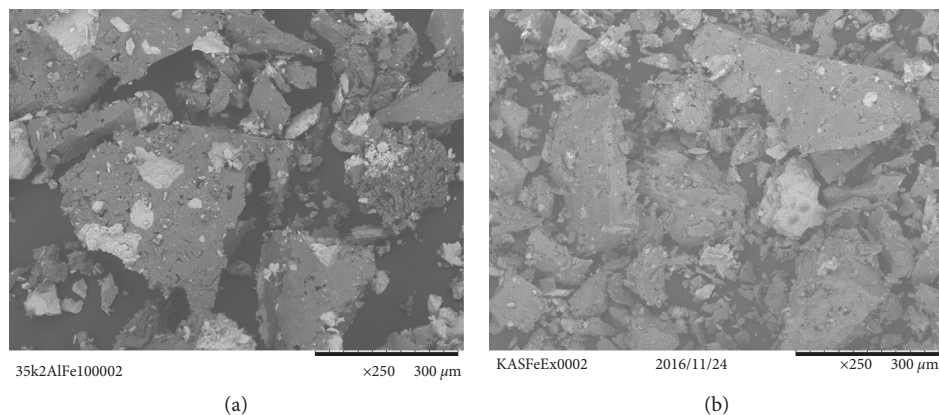


FIGURE 5: Micrographs (SEM) attained at 250 \times of the magnetic catalysts: (a) $K_2CO_3/\gamma-Al_2O_3/(0.3)Fe_3O_4$; (b) $K_2CO_3/\gamma-Al_2O_3/sepiolite/(0.3)Fe_3O_4$.

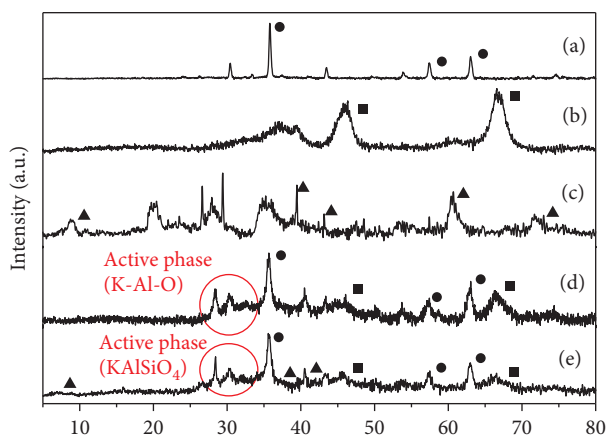


FIGURE 6: X-ray diffraction patterns for (a) Fe_3O_4 , (b) $\gamma-Al_2O_3$, (c) sepiolite, (d) $K_2CO_3/\gamma-Al_2O_3/(0.3)Fe_3O_4$ catalyst, and (e) $K_2CO_3/\gamma-Al_2O_3/sepiolite/(0.3)Fe_3O_4$ catalyst.

TABLE 4: Comparison of the catalytic performance of structured catalysts for transesterification reactions reported in the literature.

Catalysts	Reaction parameters			Biodiesel yield (%)	References
	Oil : alcohol molar ratio	Catalyst (wt.%)	Reaction conditions		
$K/BC-Fe_2O_3$ (magnetic)	Methanol (1 : 8)	2.5	60°C, 60 min, 400 rpm	98	[25]
$^a(Al_2O_3)_{8.2}(ZnO)_{2.0}$	Soybean : methanol (1 : 10)	—	100°C, 300 min	75	[48]
$^a(Al_2O_3)_{8.2}(ZnO)_{2.0}$	Soybean : ethanol (1 : 10)	—	100°C, 300 min	35	
Zr-SBA-15	Animal fat and waste cooking : methanol (1 : 50)	12.45	209°C, 360 min, 2000 rpm	92	[49]
$^bMg-Al/monoliths$	Sunflower : methanol (1 : 48)	2	60°C, 600 min	77	[50]
Zinc aluminate	Rapeseed : methanol (1 : 27)	4	200°C, 360 min, 800 rpm	70	[51]
$K/Al_2O_3-cordierite$	Soybean : methanol (1 : 32)	0.5	120°C, 360 min, 500 rpm	59	[52]
cZnL_2 structured support	Rapeseed : methanol (1 : 12)	0.3	195°C	54	[53]
$K_2CO_3/\gamma-Al_2O_3/sepiolite/(0.3)Fe_3O_4$	Sunflower : ethanol (1 : 12)	5	78°C, 240 min, 200 rpm	≈88	In this study

^aReaction carried out in a fixed-bed tubular reactor. ^bMg-Al hydrotalcites Fecralloy[®] monoliths used as supports—reaction carried out at 1 atm. ^cReaction carried out at 20 bars.

Data Availability

The data used to support the findings of this study are available from the corresponding author upon request.

Conflicts of Interest

The authors declare that they have no conflicts of interest.

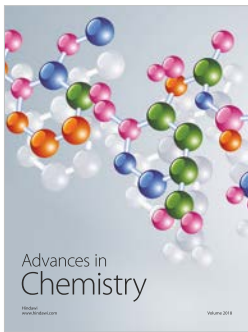
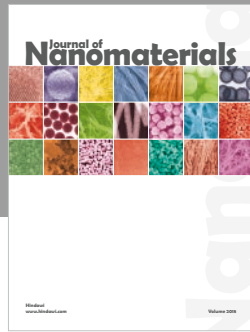
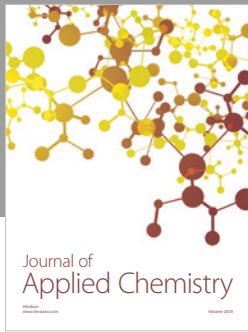
Acknowledgments

We are grateful to the Programme of the Madrid Community ALCCONES, S2013/MAE-2985; the Spanish Ministry Grant CTM2017-82335-R “RIEN2O”; Natural Sciences Graduate Program from the State University of Northern of Rio de Janeiro for the Postdoctoral Position Grants (No. 001/2017); Carlos Chagas Filho Research Foundation of the Rio de Janeiro State (FAPERJ Process No. E-26/210.508/2014); National Council for Scientific and Technological Development (CNPq Process No. 311942/2015-6); and Coordination for the Improvement of Higher-Level Personnel-Brazil (CAPES Finance Code 001) for the financial support.

References

- [1] ANP (National Agency of Petroleum, Natural Gas and Biofuels), *Monthly Bulletin of Biodiesel*, ANP, Rio de Janeiro, Brazil, 2017, <http://www.anp.gov.br/publicacoes/boletins-anp/2386-boletim-mensal-do-biodiesel>.
- [2] ANP (National Agency of Petroleum, Natural Gas and Biofuels), *Mandatory Percentage of Biodiesel Increases to 10%*, ANP, Rio de Janeiro, Brazil, 2018, <http://www.anp.gov.br/noticias/4333-percentual-obrigatorio-de-biodiesel-passa-para-10>.
- [3] V. H. Perez, E. G. Silveira Jr., D. C. Cubides et al., “Trends in biodiesel production: present status and future directions,” in *Biofuels in Brazil*, pp. 281–302, Springer Science & Business Media, Berlin, Germany, 2014.
- [4] E. G. Silveira Junior, E. Simionatto, V. H. Perez, O. R. Justo, N. A. H. Zárate, and M. D. C. Vieira, “Potential of Virginia-type peanut (*Arachis hypogaea* L.) as feedstock for biodiesel production,” *Industrial Crops and Products*, vol. 89, pp. 448–454, 2016.
- [5] A. Galadima and O. Muraza, “Biodiesel production from algae by using heterogeneous catalysts: a critical review,” *Energy*, vol. 78, pp. 72–83, 2014.
- [6] K. Neumann, K. Werth, A. Martín, and A. Górak, “Biodiesel production from waste cooking oils through esterification: catalyst screening, chemical equilibrium and reaction kinetics,” *Chemical Engineering Research and Design*, vol. 107, pp. 52–62, 2015.
- [7] ANP (National Agency of Petroleum, Natural Gas and Biofuels), “Dados estatísticos,” December 2018, <http://www.anp.gov.br/dados-estatisticos>.
- [8] A. S. Yusuff, O. D. Adeniyi, M. A. Olutoye, and U. G. Akpan, “A review on application of heterogeneous catalyst in the production of biodiesel from vegetable oils,” *Journal of Applied Science & Process Engineering*, vol. 4, pp. 142–157, 2017.
- [9] B. Singh, A. Guldhe, I. Rawat, and F. Bux, “Towards a sustainable approach for development of biodiesel,” *Renewable and Sustainable Energy Reviews*, vol. 29, pp. 216–245, 2014.
- [10] I. Korkut and M. Bayramoglu, “Selection of catalyst and reaction conditions for ultrasound assisted biodiesel production from canola oil,” *Renewable Energy*, vol. 116, pp. 543–551, 2018.
- [11] I. Reyeró, G. Arzamendi, and L. M. Gandía, “Heterogenization of the biodiesel synthesis catalysis: CaO and novel calcium compounds as transesterification catalysts,” *Chemical Engineering Research and Design*, vol. 92, no. 8, pp. 1519–1530, 2014.
- [12] M. Kouzu, T. Kasuno, M. Tajika, S. Yamanaka, and J. Hidaka, “Active phase of calcium oxide used as solid base catalyst for transesterification of soybean oil with refluxing methanol,” *Applied Catalysis A: General*, vol. 334, no. 1–2, pp. 357–365, 2008.
- [13] C. C. A. Loures, M. S. Amaral, P. C. M. Da Rós, S. M. F. E. Zorn, H. F. de Castro, and M. B. Silva, “Simultaneous esterification and transesterification of microbial oil from *Chlorella minutissima* by acid catalysis route: a comparison between homogeneous and heterogeneous catalysts,” *Fuel*, vol. 211, pp. 261–268, 2018.
- [14] A. K. F. Carvalho, L. R. V. da Conceição, J. P. V. Silva, V. H. Perez, and H. F. de Castro, “Biodiesel production from *Mucor circinelloides* using ethanol and heteropolyacid in one and two-step transesterification,” *Fuel*, vol. 202, pp. 503–511, 2017.
- [15] S. K. Kundu and A. Bhaumik, “Pyrene-based porous organic polymers as efficient catalytic support for the synthesis of biodiesels at room temperature,” *ACS Sustainable Chemistry & Engineering*, vol. 3, no. 8, pp. 1715–1723, 2015.
- [16] S. Bhunia, B. Banerjee, and A. Bhaumik, “A new hyper-crosslinked supermicroporous polymer, scope for sulfonation and its catalytic potential for the efficient synthesis of biodiesel at room temperature,” *Chemical Communications*, vol. 51, no. 24, pp. 5020–5023, 2015.
- [17] N. Mansir, S. Hwa, U. Rashid, M. Izham, and Y. Ping, “Modified waste egg shell derived bifunctional catalyst for biodiesel production from high FFA waste cooking oil. A review,” *Renewable and Sustainable Energy Reviews*, vol. 82, pp. 3645–3655, 2018.
- [18] M. Farooq, A. Ramli, and D. Subbarao, “Biodiesel production from waste cooking oil using bifunctional heterogeneous solid catalysts Original,” *Journal of Cleaner Production*, vol. 59, pp. 131–140, 2013.
- [19] P. Rós, C. Silva, M. Silva-Stenico, M. Fiore, and H. Castro, “Microbial oil derived from filamentous cyanobacterium *trichormus* sp. as feedstock to yield fatty acid ethyl esters by enzymatic synthesis,” *Journal of Advances in Biology & Biotechnology*, vol. 12, no. 4, pp. 1–14, 2017.
- [20] A. B. R. Moreira, V. H. Perez, G. M. Zanin, and H. F. de Castro, “Biodiesel synthesis by enzymatic transesterification of palm oil with ethanol using lipases from several sources immobilized on silica-PVA composite,” *Energy and Fuels*, vol. 21, no. 6, pp. 3689–3694, 2007.
- [21] A. L. De Lima, C. M. Ronconi, and C. J. A. Mota, “Heterogeneous basic catalysts for biodiesel production,” *Catalysis Science & Technology*, vol. 6, no. 9, pp. 2877–2891, 2016.
- [22] C. G. C. M. Netto, H. E. Toma, and L. H. Andrade, “Superparamagnetic nanoparticles as versatile carriers and supporting materials for enzymes,” *Journal of Molecular Catalysis B: Enzymatic*, vol. 85–86, pp. 71–92, 2013.
- [23] W. Xie and X. Zang, “Immobilized lipase on core-shell structured Fe₃O₄-MCM-41 nanocomposites as a magnetically recyclable biocatalyst for interesterification of soybean oil and lard,” *Food Chemistry*, vol. 194, pp. 1283–1292, 2016.
- [24] W. Xie and F. Wan, “Basic ionic liquid functionalized magnetically responsive Fe₃O₄@ HKUST-1 composites

- used for biodiesel production,” *Fuel*, vol. 220, pp. 248–256, 2018.
- [25] K. Liu, R. Wang, and M. Yu, “An efficient, recoverable solid base catalyst of magnetic bamboo charcoal: preparation, characterization, and performance in biodiesel production,” *Renewable Energy*, vol. 127, pp. 531–538, 2018.
- [26] Ž. Kesić, I. Lukić, M. Zdujić, Č. Jovalekić, V. Veljković, and D. Skala, “Assessment of CaTiO_3 , CaMnO_3 , CaZrO_3 and $\text{Ca}_2\text{Fe}_2\text{O}_5$ perovskites as heterogeneous base catalysts for biodiesel synthesis,” *Fuel Processing Technology*, vol. 143, pp. 162–168, 2016.
- [27] Y. Liu, P. Zhang, M. Fan, and P. Jiang, “Biodiesel production from soybean oil catalyzed by magnetic nanoparticle $\text{MgFe}_2\text{O}_4/\text{CaO}$,” *Fuel*, vol. 164, pp. 314–321, Jan. 2016.
- [28] B. Chang, Y. Li, Y. Guo, and B. Yang, “Journal of the Taiwan Institute of Chemical Engineers simple fabrication of magnetically separable mesoporous carbon sphere with excellent catalytic performance for biodiesel production,” *Journal of the Taiwan Institute of Chemical Engineers*, vol. 60, pp. 241–246, 2016.
- [29] F. Zhang, Z. Fang, and Y. Wang, “Biodiesel production directly from oils with high acid value by magnetic $\text{Na}_2\text{SiO}_3/\text{Fe}_3\text{O}_4/\text{C}$ catalyst and ultrasound,” *Fuel*, vol. 150, pp. 370–377, 2015.
- [30] B. Xue, J. Luo, F. Zhang, and Z. Fang, “Biodiesel production from soybean and *Jatropha* oils by magnetic CaFe_2O_4 – CaFe_2O_5 -based catalyst,” *Energy*, vol. 68, pp. 584–591, 2014.
- [31] M. B. Alves, F. C. M. Medeiros, M. H. Sousa, J. C. Rubim, and P. A. Z. Suarez, “Cadmium and tin magnetic nanocatalysts useful for biodiesel production,” *Journal of the Brazilian Chemical Society*, vol. 25, pp. 2304–2313, 2014.
- [32] G. F. Cubides-Roman, V. H. Pérez, H. F. de Castro et al., “Ethyl esters (biodiesel) production by *Pseudomonas fluorescens* lipase immobilized on chitosan with magnetic properties in a bioreactor assisted by electromagnetic field,” *Fuel*, vol. 196, pp. 481–487, 2017.
- [33] G. Chen, J. Liu, J. Yao, Y. Qi, and B. Yan, “Biodiesel production from waste cooking oil in a magnetically fluidized bed reactor using whole-cell biocatalysts,” *Energy Conversion and Management*, vol. 138, pp. 556–564, 2017.
- [34] M. Hajar and F. Vahabzadeh, “Biolubricant production from castor oil in a magnetically stabilized fluidized bed reactor using lipase immobilized on Fe_3O_4 nanoparticles,” *Industrial Crops and Products*, vol. 94, pp. 544–556, 2016.
- [35] G.-X. Zhou, G. Chen, and B. Yan, “Biodiesel production in a magnetically-stabilized, fluidized bed reactor with an immobilized lipase in magnetic chitosan microspheres,” *Biotechnology Letters*, vol. 36, no. 1, pp. 63–68, 2014.
- [36] ASTM D4179-82, *Standard Test Method for Single Pellet Crush Strength of Formed Catalyst Shapes 1*, Vol.14, ASTM International, West Conshohocken, PA, USA, 2001.
- [37] S. Brunauer, P. H. Emmett, and E. Teller, “Adsorption of gases in multimolecular layers,” *Journal of the American Chemical Society*, vol. 60, no. 2, pp. 309–319, 1938.
- [38] E. P. Barret, L. G. Joyner, and P. P. Halenda, “The determination of pore volume and area distributions in porous substances. I. Computations from nitrogen isotherms,” *Journal of the American Chemical Society*, vol. 73, no. 1, pp. 373–380, 1951.
- [39] S. Yamadaya, M. Oba, and T. Hasegawa, “The mechanical strength of heterogeneous catalyst I. The tensile strength of pelletized alumina catalysts,” *Journal of Catalysis*, vol. 270, pp. 264–270, 1970.
- [40] J. Chandradass and M. Balasubramanian, “Sol-gel processing of alumina fibres,” *Journal of Materials Processing Technology*, vol. 173, no. 3, pp. 275–280, 2006.
- [41] H. Nagata, S. Shimoda, and T. Sudo, “On dehydration of bound water of sepiolite,” *Clays and Clay Minerals*, vol. 22, no. 3, pp. 285–293, 1974.
- [42] R. L. Frost and Z. Ding, “Controlled rate thermal analysis and differential scanning calorimetry of sepiolites and palygorskites,” *Thermochimica Acta*, vol. 397, no. 1-2, pp. 119–128, 2003.
- [43] S. Hojati and H. Khademi, “Thermal behavior of a natural sepiolite from Northeastern Iran,” *Journal of Sciences, Islamic Republic of Iran*, vol. 24, pp. 129–134, 2013.
- [44] P. Avila, J. Blanco, A. Bahamonde, J. M. Palacios, and C. Barthelemy, “Influence of the binder on the properties of catalysts based on titanium-vanadium oxides,” *Journal of Materials Science*, vol. 28, no. 15, pp. 4113–4118, 1993.
- [45] S. B. Rasmussen, J. Due-Hansen, M. Villarroel, F. J. Gil-Llambias, R. Fehrmann, and P. Ávila, “Multidisciplinary determination of the phase distribution for $\text{VOX-ZrO}_2\text{-SO}_4^{2-}$ -sepiolite catalysts for $\text{NH}_3\text{-SCR}$,” *Catalysis Today*, vol. 172, no. 1, pp. 73–77, 2011.
- [46] H. Wu, Y. Liu, J. Zhang, and G. Li, “Bioresource technology in situ reactive extraction of cottonseeds with methyl acetate for biodiesel production using magnetic solid acid catalysts,” *Bioresource Technology*, vol. 174, pp. 182–189, 2014.
- [47] S. Tang, L. Wang, Y. Zhang, S. Li, S. Tian, and B. Wang, “Study on preparation of $\text{Ca/Al/Fe}_3\text{O}_4$ magnetic composite solid catalyst and its application in biodiesel transesterification,” *Fuel Processing Technology*, vol. 95, pp. 84–89, 2012.
- [48] F. M. da Silva, D. M. M. Pinho, G. P. Houg et al., “Continuous biodiesel production using a fixed-bed Lewis-based catalytic system,” *Chemical Engineering Research and Design*, vol. 92, no. 8, pp. 1463–1469, 2014.
- [49] J. Iglesias, J. A. Melero, L. F. Bautista, G. Morales, and R. Sánchez-Vázquez, “Continuous production of biodiesel from low grade feedstock in presence of Zr-SBA-15: catalyst performance and resistance against deactivation,” *Catalysis Today*, vol. 234, pp. 174–181, 2014.
- [50] I. Reyero, I. Velasco, O. Sanz, M. Montes, G. Arzamendi, and L. M. Gandía, “Structured catalysts based on Mg–Al hydrotalcite for the synthesis of biodiesel,” *Catalysis Today*, vol. 216, pp. 211–219, 2013.
- [51] V. Pugno, S. Maury, V. Coupard et al., “Stability, activity and selectivity study of a zinc aluminate heterogeneous catalyst for the transesterification of vegetable oil in batch reactor,” *Applied Catalysis A: General*, vol. 374, no. 1-2, pp. 71–78, 2010.
- [52] G. M. Tonetto and J. M. Marchetti, “Transesterification of soybean oil over $\text{Me/Al}_2\text{O}_3$ ($\text{Me} = \text{Na, Ba, Ca, and K}$) catalysts and monolith $\text{K/Al}_2\text{O}_3$ -cordierite,” *Topics in Catalysis*, vol. 53, no. 11-12, pp. 755–762, 2010.
- [53] S. T. Kolaczowski, U. A. Asli, and M. G. Davidson, “A new heterogeneous ZnL_2 catalyst on a structured support for biodiesel production,” *Catalysis Today*, vol. 147, pp. 220–224, 2009.



Hindawi
Submit your manuscripts at
www.hindawi.com

